

1 Supplemental Information for

2

3 **Bomb-radiocarbon signal suggests that soil carbon**  
4 **contributes to chlorophyll *a* in archival oak leaves**

5

6 Naoto F. Ishikawa<sup>1, 2, †</sup>, Hisami Suga<sup>1</sup>, Tessa S. van der Voort<sup>2</sup>, Reto Nyffeler<sup>3</sup>, Nanako O.

7 Ogawa<sup>1</sup>, Negar Haghipour<sup>2, 4</sup>, Lukas Wacker<sup>4</sup>, Timothy I. Eglinton<sup>2</sup> and, Naohiko Ohkouchi<sup>1</sup>

8

9 <sup>1</sup>Japan Agency for Marine-Earth Science and Technology, Yokosuka 237-0061, Japan

10 <sup>2</sup>Department of Earth Sciences, ETH Zürich, 8092 Zürich, Switzerland

11 <sup>3</sup>Department of Systematic and Evolutionary Botany, University of Zürich, 8008 Zürich,  
12 Switzerland

13 <sup>4</sup>Laboratory for Ion Beam Physics, ETH Zürich, 8093 Zürich, Switzerland

14

15 <sup>†</sup>Corresponding author. E-mail: ishikawan@jamstec.go.jp

16 Running head:  $\Delta^{14}\text{C}$  of chlorophyll *a* in archival oak leaves

17

18 **Supplemental Text**

19 To identify and characterize impurity carbon in the purified Pheo *a* fractions, three additional  
20 assessments based on (i) diode array detector (DAD), (ii) Orbitrap MS, and (iii) GC/MS  
21 spectra were performed. Assessment (i) was subject to all eight samples, while assessment (ii)  
22 subject to 1952, 1968, 1973, 1982, and 1995 samples and assessment (iii) subject to 1952 and  
23 1968 samples due to availability of leftover materials after CSRA.

24

25 *(i) DAD spectrum*

26 The DAD spectrum of all samples spanning from 300 to 720 nm absorbance was examined at  
27 the time window between 16.5 to 20.5 min when the Pheo *a* allomer, Pheo *a*, and Pheo *a*  
28 epimer were collected by fraction collector. The HPLC setting was the same as the second-  
29 step separation using Eclipse PAH column. Exogeneous compounds having absorbance at the  
30 300–720 nm range were not found (Figure S1). Based on peak areas at 660 nm of Pheo *a*  
31 allomer, Pheo *a*, and Pheo *a* epimer, their relative proportion in each sample was estimated  
32 (Figure S2).

33

34 *(ii) Orbitrap MS spectrum*

35 Selected samples (1952, 1968, 1973, 1982, and 1995 CE) were injected to an UltiMate 3000  
36 and Q Exactive™ Plus Hybrid Quadrupole-Orbitrap™ mass spectrometer (Thermo Fischer  
37 Scientific Inc., Waltham, MA, USA) using the electrospray ionization (ESI) method under an  
38 infusion mode. Exogeneous compounds that were ionized by ESI were not found except for  
39 Pheo *a* allomers (allomer 1:  $m/z$  887.6,  $\text{C}_{55}\text{H}_{74}\text{N}_4\text{O}_6$ , allomer 2:  $m/z$  903.6,  $\text{C}_{55}\text{H}_{74}\text{N}_4\text{O}_7$ ,  
40 allomer 3:  $m/z$  919.6,  $\text{C}_{55}\text{H}_{74}\text{N}_4\text{O}_8$ , allomer 4:  $m/z$  935.6,  $\text{C}_{55}\text{H}_{74}\text{N}_4\text{O}_9$ ) (Figure S3). The  
41 addition of oxygen to the Pheo *a* compound likely occurred in sample preparation and/or  
42 storage process due to an exposure to ambient air, which does not increase its C/N nor affect

43 sample purity for CSRA measurements. Based on peak areas at exact *m/z* of Pheo *a* and its  
44 allomers, their relative proportion in each sample was estimated (Figure S4). There was a  
45 strong positive correlation in proportions of Pheo *a* allomers between DAD-based estimates  
46 and Orbitrap MS-based estimates (Figure S5).

47

48 *(iii) GC/MS spectrum*

49 Selected samples (1952 and 1968CE) were dissolved in *n*-hexane, and loaded on deactivated  
50 1 % H<sub>2</sub>O silica gel columns pre-conditioned with hexane. The N-1, N-2, and N-3 fractions  
51 were extracted with *n*-hexane, *n*-hexane/dichloromethane (50:50, v/v), and  
52 dichloromethane/methanol (90:10, v/v) respectively. After drying with argon gas, these  
53 fractions were redissolved in *n*-hexane/dichloromethane and were injected to a gas  
54 chromatograph/mass spectrometer (GC/MS) (Agilent 7890A-GC with Agilent 5975C inert  
55 XL MSD) equipped with the VF-5ms column (0.25 mm ×30 m, film thickness 0.10 μm) with  
56 the electron ionization (EI) method (70eV). The oven temperature was programmed as  
57 follows: maintained at 40 °C for 2 min, raised up to 120 °C at 30 °C min<sup>-1</sup>, then to 320 °C at  
58 6 °C min<sup>-1</sup>, and maintained at 320 °C for 20 min. Helium was used as the carrier gas with a  
59 constant flow are of 1 mL min<sup>-1</sup>.

60 For the N-1 and N-2 fractions, no peaks were found. For the N-3 fraction, peaks  
61 around 12–13 min appeared both in the in-house Pheo *a* standard and the samples, suggesting  
62 that these are ionized fractions of Pheo *a* compound. Exogeneous compounds that were  
63 ionized by EI were not found except for pentacyclic triterpenoid compounds (β-amyrin,  
64 simiarenol, and their derivatives) eluting around 31–32 min, which were identified by mass  
65 fragment patterns (Elgamal *et al.*, 1969; Galeron *et al.*, 2016; Shiojima *et al.*, 1992). (Figures  
66 S6–S13).

67

68 **Supplemental References**

69 Elgamal, M. H. A., Favez, M. B. E., & Kemp, T. R. (1969). The mass spectra of some  
70 triterpenoid dehydration products. *Organic Mass Spectrometry*, 2(2), 175–194.  
71 <https://doi.org/10.1002/oms.1210020204>

72 Galeron, M. A., Vaultier, F., & Rontani, J. F. (2016). Oxidation products of  $\alpha$ - And  $\beta$ -  
73 amyrins: Potential tracers of abiotic degradation of vascular-plant organic matter in  
74 aquatic environments. *Environmental Chemistry*, 13(4), 732–744.  
75 <https://doi.org/10.1071/EN15237>

76 Shiojima, K., Arai, Y., Masuda, K., Takase, Y., Ageta, T., & Ageta, H. (1992). Mass Spectra  
77 of Pentacyclic Triterpenoids. *Chemical and Pharmaceutical Bulletin*, 40(7), 1683–1690.  
78 <https://doi.org/10.1248/cpb.40.1683>

79

80

81 **FIGURE LEGENDS**

82 Figure S1. HPLC/DAD spectrums of Pheo *a* collected through separation using the C18 (1st)  
83 and PAH (2nd) columns in (a) 1952 CE, (b) 1965 CE, (c) 1966 CE, (d) 1968 CE, (e) 1973  
84 CE, (f) 1982 CE, (g) 1995 CE, and (h) 2007 CE. Dashed lines indicate fraction collection  
85 window (16.5–20.5 min).

86

87 Figure S2. DAD peak area (660 nm) percentage of Pheo *a* allomer (16.5–17.8 min), Pheo *a*  
88 allomer epimer, Pheo *a* (17.8–19.2 min), and Pheo *a* epimer (19.2–20.5 min).

89

90 Figure S3. Orbitrap MS chromatograms of Pheo *a* ( $m/z$  871.6,  $\text{C}_{55}\text{H}_{74}\text{N}_4\text{O}_5$ ) in (a) an in-house  
91 standard, (b) 1952 CE, (c) 1968 CE, (d) 1973 CE, (e) 1982 CE, and (f) 1995 CE.

92

93 Figure S4. Orbitrap MS peak area percentage of Pheo *a* and its allomers.

94

95 Figure S5. Relationship between DAD peak area (660 nm) percentage and Orbitrap MS peak  
96 area percentage of Pheo *a* and its allomers. The strong positive correlation corroborates that  
97 the compounds are Pheo *a* derivatives (allomers).

98

99 Figure S6. Total ion chromatogram of the N-3 fraction (a) in an in-house standard Pheo *a* and  
100 (b) in Pheo *a* extracted from the *Quercus pubescens* leaf collected in 1952 CE and purified for  
101 CSRA.

102

103 Figure S7. (a) Total ion chromatogram and (b) mass spectrum of the first unknown peak of  
104 the N-3 fraction in Pheo *a* in 1952 CE. The asterisk denotes the peak for which the mass  
105 spectrum is obtained.

106

107 Figure S8. (a) Total ion chromatogram and (b) mass spectrum of the second unknown peak of  
108 the N-3 fraction in Pheo *a* in 1952 CE. The asterisk denotes the peak for which the mass  
109 spectrum is obtained.

110

111 Figure S9. (a) Total ion chromatogram and (b) mass spectrum of the third unknown peak of  
112 the N-3 fraction in Pheo *a* in 1952 CE. The asterisk denotes the peak for which the mass  
113 spectrum is obtained.

114

115 Figure S10. Total ion chromatogram of the N-3 fraction (a) in an in-house standard Pheo *a*  
116 and (b) in Pheo *a* extracted from the *Quercus pubescens* leaf collected in 1968 CE and  
117 purified for CSRA.

118

119 Figure S11. (a) Total ion chromatogram and (b) mass spectrum of the first unknown peak of  
120 the N-3 fraction in Pheo *a* in 1968 CE. The asterisk denotes the peak for which the mass  
121 spectrum is obtained.

122

123 Figure S12. (a) Total ion chromatogram and (b) mass spectrum of the second unknown peak  
124 of the N-3 fraction in Pheo *a* in 1968 CE. The asterisk denotes the peak for which the mass  
125 spectrum is obtained.

126

127 Figure S13. (a) Total ion chromatogram and (b) mass spectrum of the third unknown peak of  
128 the N-3 fraction in Pheo *a* in 1968 CE. The asterisk denotes the peak for which the mass  
129 spectrum is obtained.

130

131 Figure S14. The observed C/N ratios (right axis in red) and blank carbon % (left axis in blue)  
132 for Chl *a* purified from *Quercus* leaf samples plotted against collection year CE. Error bars  
133 indicate  $1\sigma$  uncertainties. The dashed red line indicates expected C/N ratios of Chl *a* (11.8).  
134 The four older samples collected in 1952, 1965, 1966, and 1968 CE showed significantly  
135 higher C/N and blank carbon % than 11.8 and 0, respectively, while the four newer samples  
136 collected in 1973, 1982, 1995, and 2007 CE did not.

137

138 Figure S15. Heatmaps of the difference ( $\Delta\Delta^{14}\text{C}$ ) between observed and modelled  $\Delta^{14}\text{C}_{\text{Chl}}$   
139 values on a biplot for soil turnover time ( $T_s$ , years) versus soil proportion ( $P_s$ , %) for each of  
140 the eight samples collected in different years. The  $\Delta\Delta^{14}\text{C}$  value larger than the  $2\sigma$  analytical  
141 error of CSRA ( $>16\text{\%}$ ) was not considered in this plot. The white arrows denote the smallest  
142  $\Delta\Delta^{14}\text{C}$  values (i.e., the most plausible models).

143

144 Figure S16. The  $\Delta\Delta^{14}\text{C}$  heatmap that overlayed all the eight heatmaps in Figure S12. The  
145 arithmetic mean of the  $\Delta\Delta^{14}\text{C}$  values from the eight years are shown. The white arrow denotes  
146 the smallest  $\Delta\Delta^{14}\text{C}$  value (i.e., the most plausible model).

147



148

149 Figure S1a

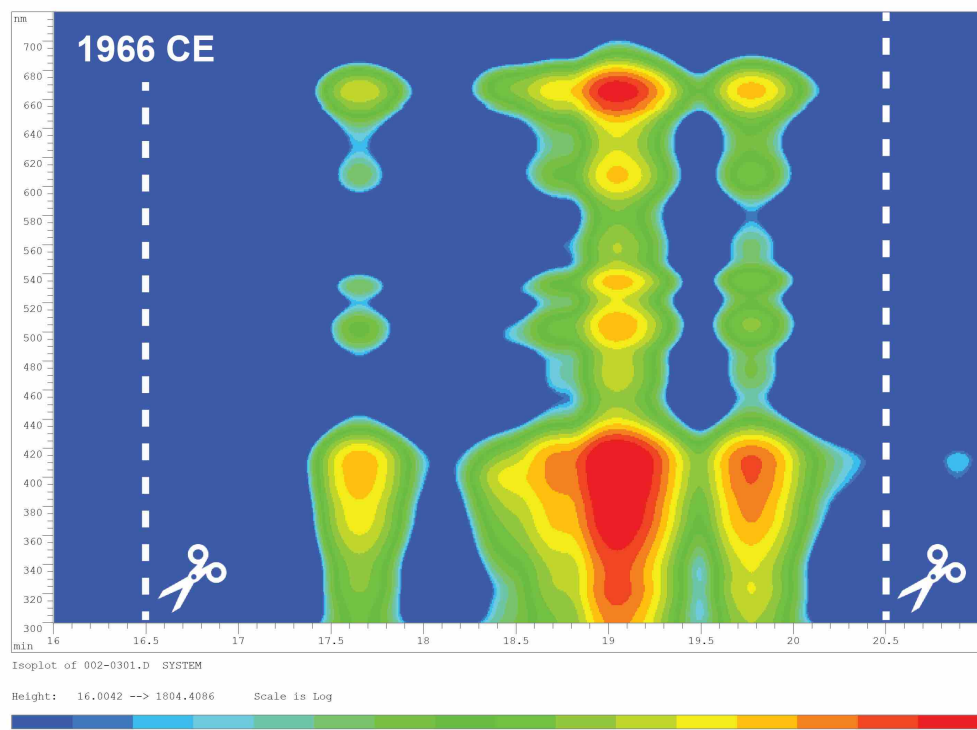
150



151

152 Figure S1b

153



154

155 Figure S1c

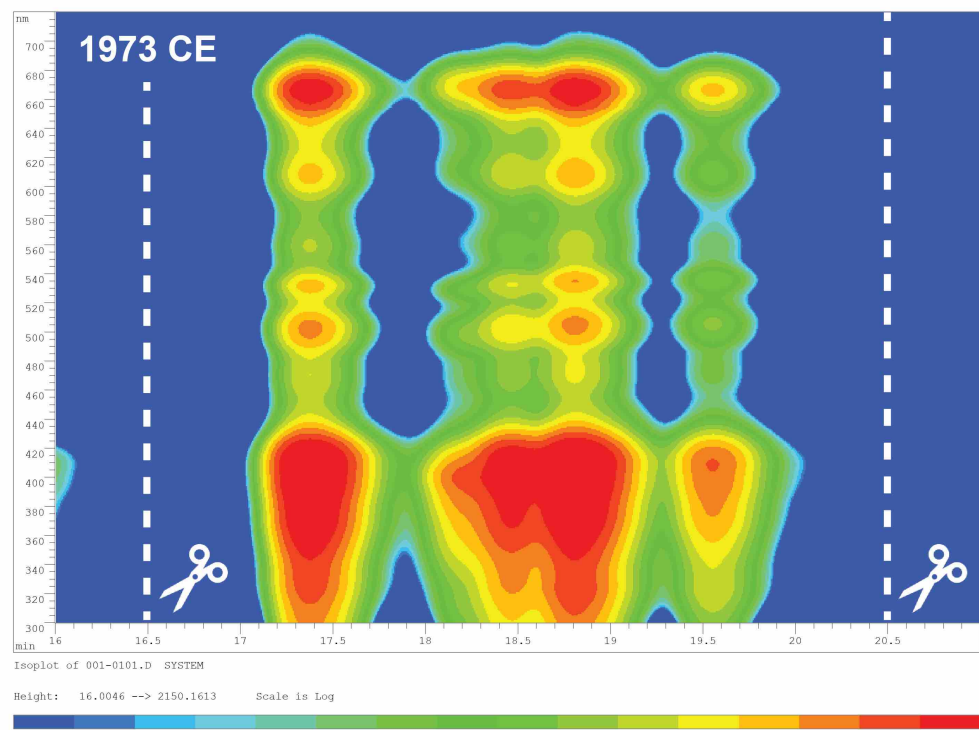
156



157

158 Figure S1d

159



160

161 Figure S1e

162



163

164 Figure S1f

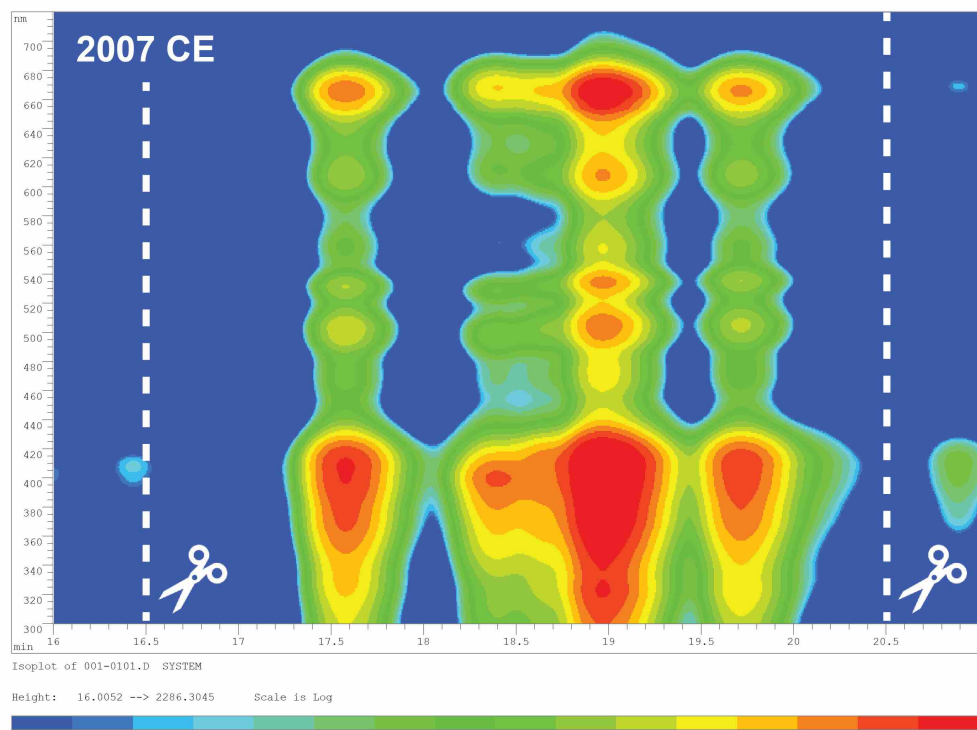
165



166

167 Figure S1g

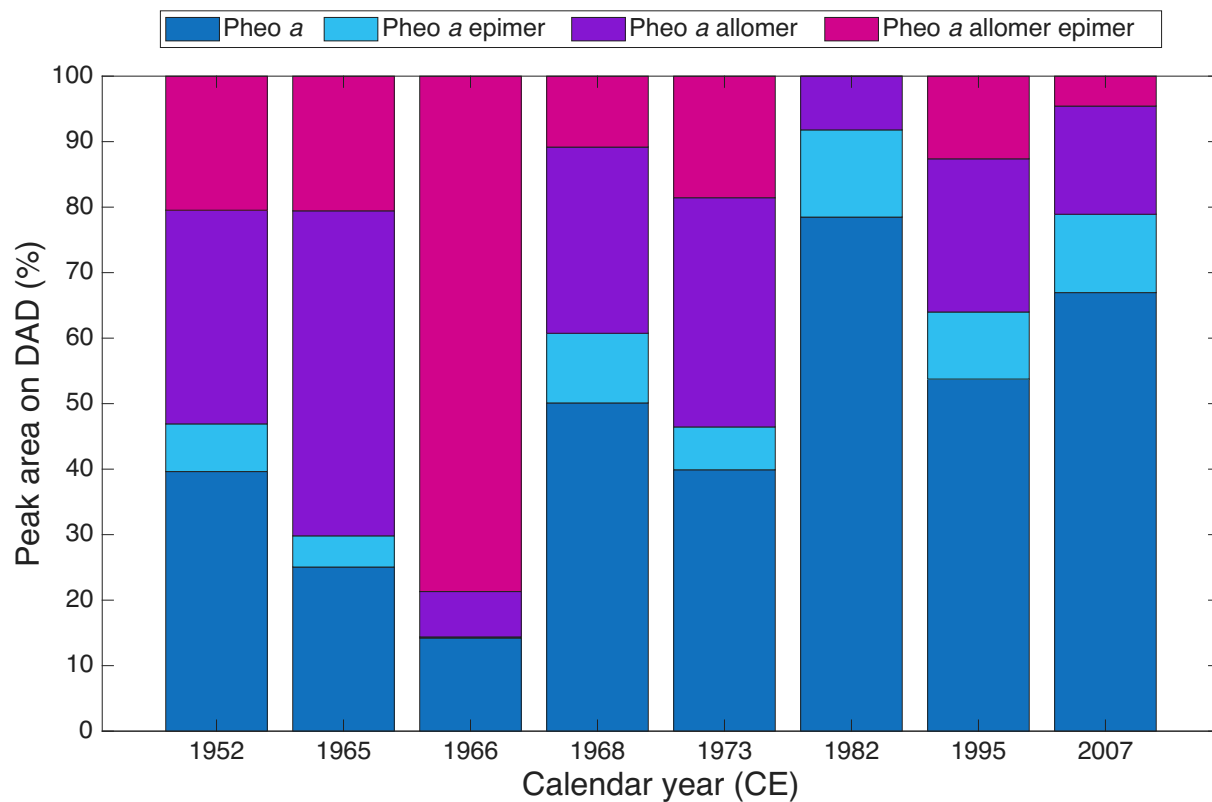
168



169

170 Figure S1h

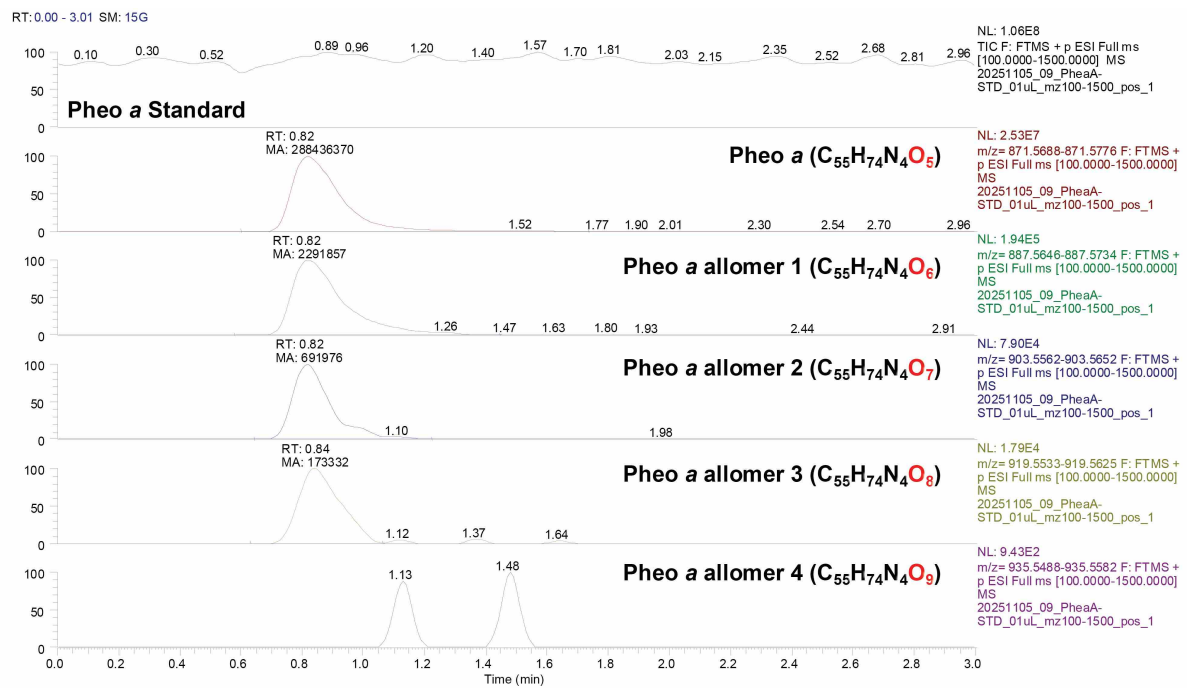
171



172

173 Figure 2

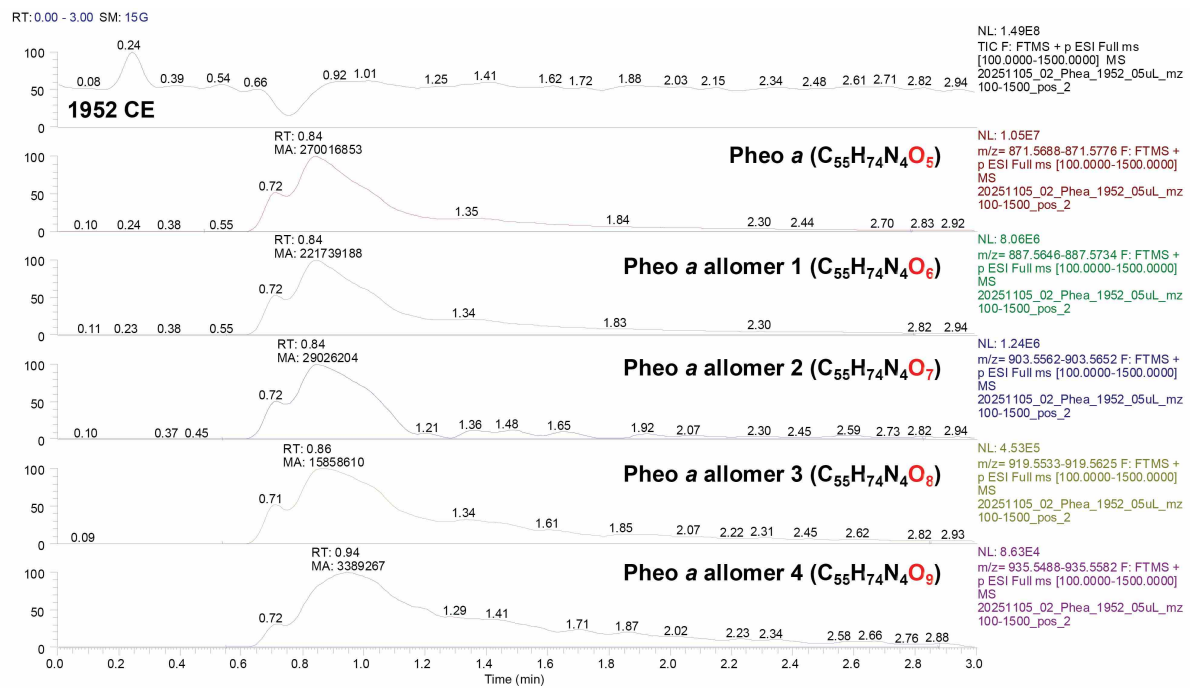
174

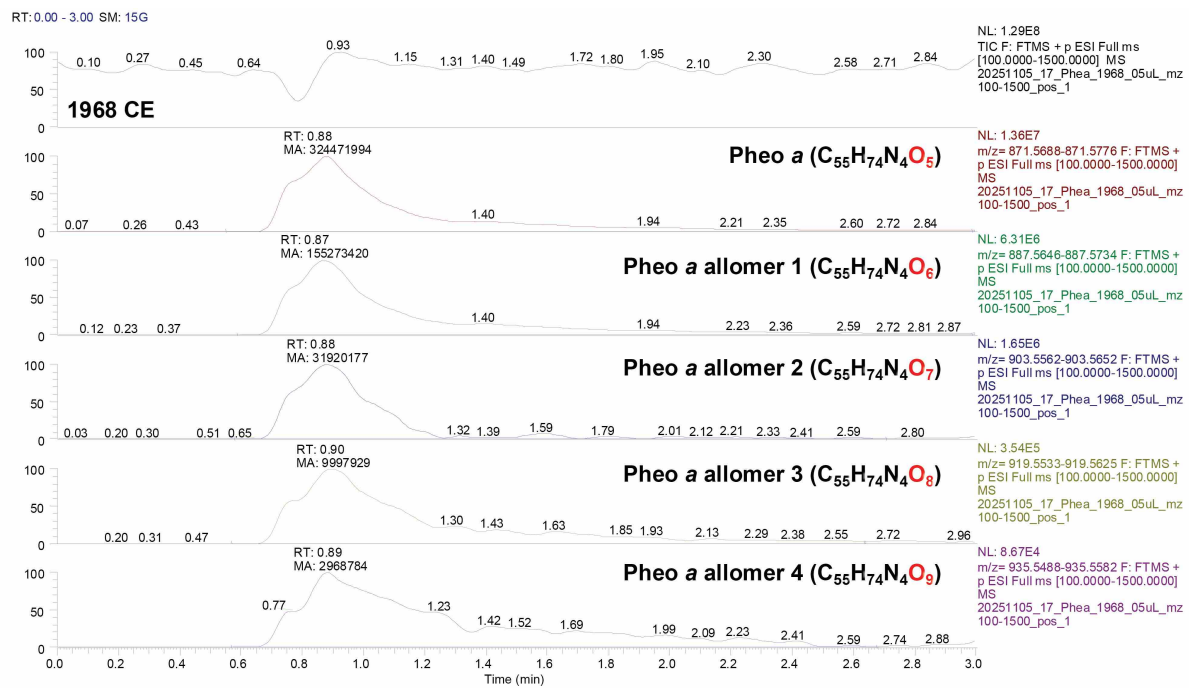


175

176 Figure S3a

177

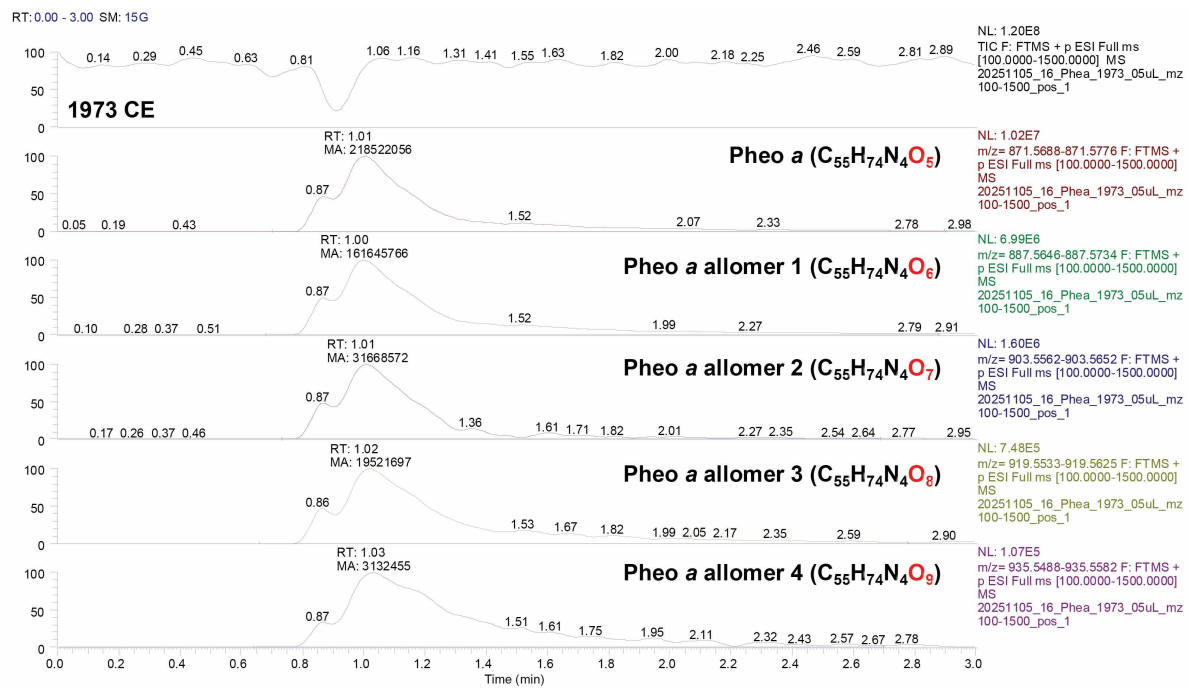




181

182 Figure S3c

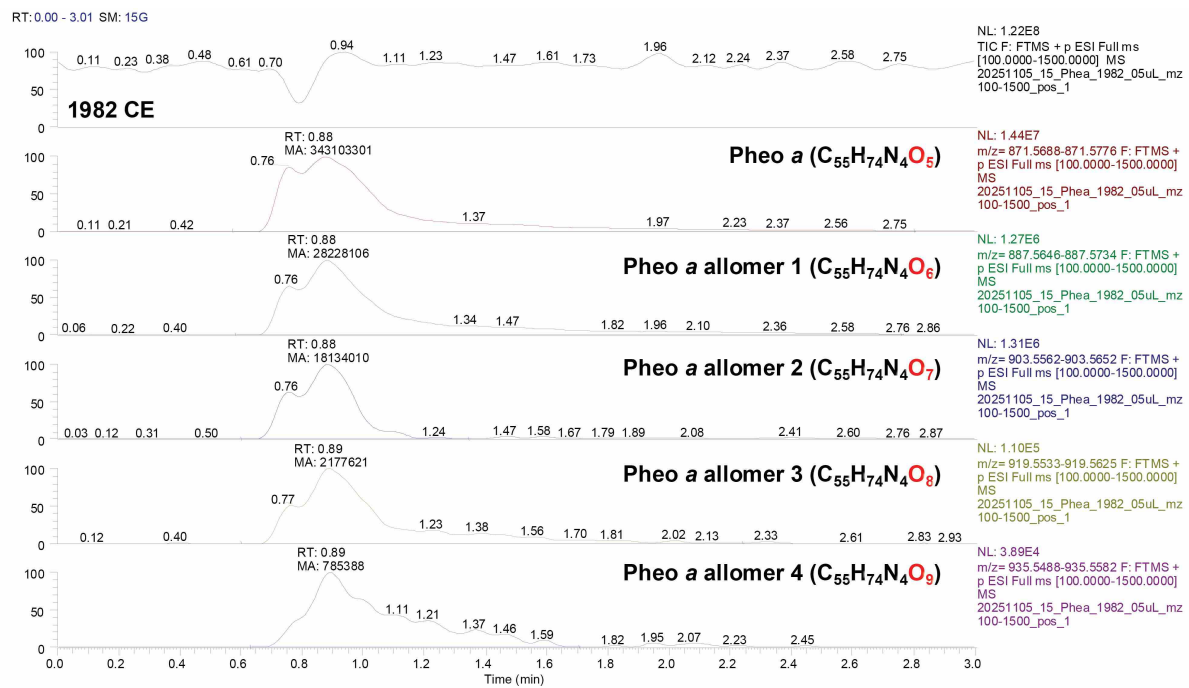
183



184

185 Figure S3d

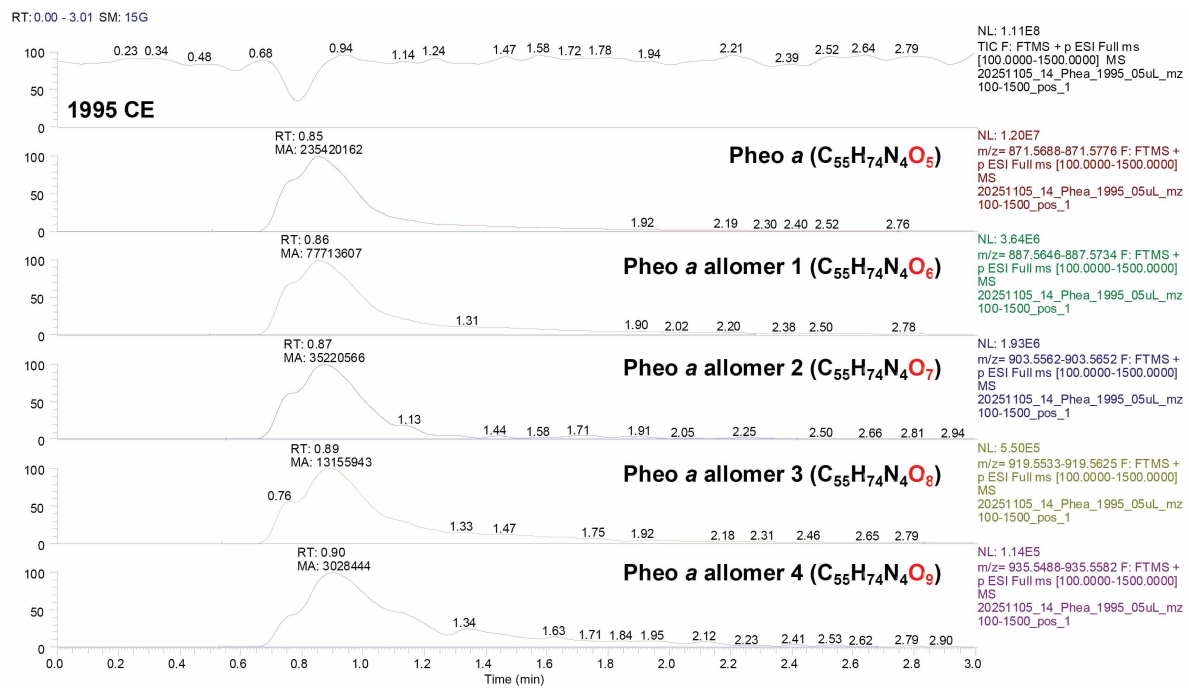
186



187

188 Figure S3e

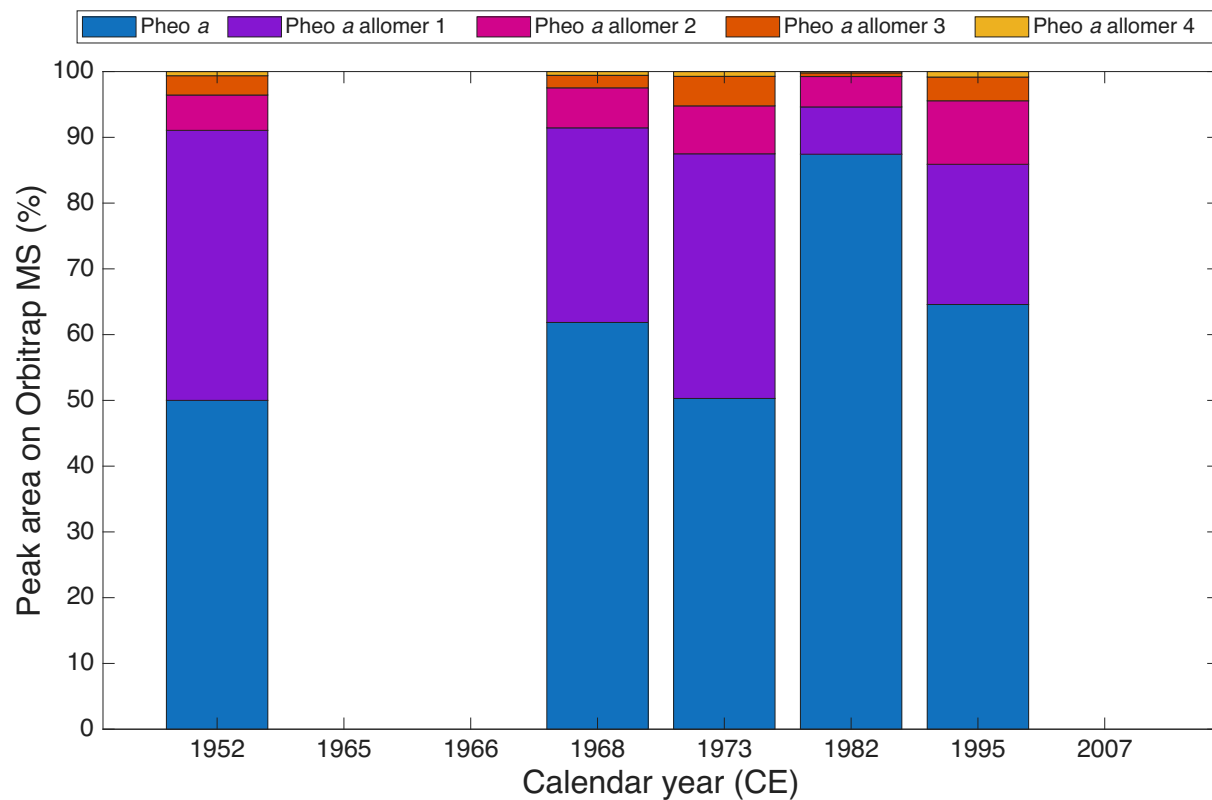
189



190

191 Figure S3f

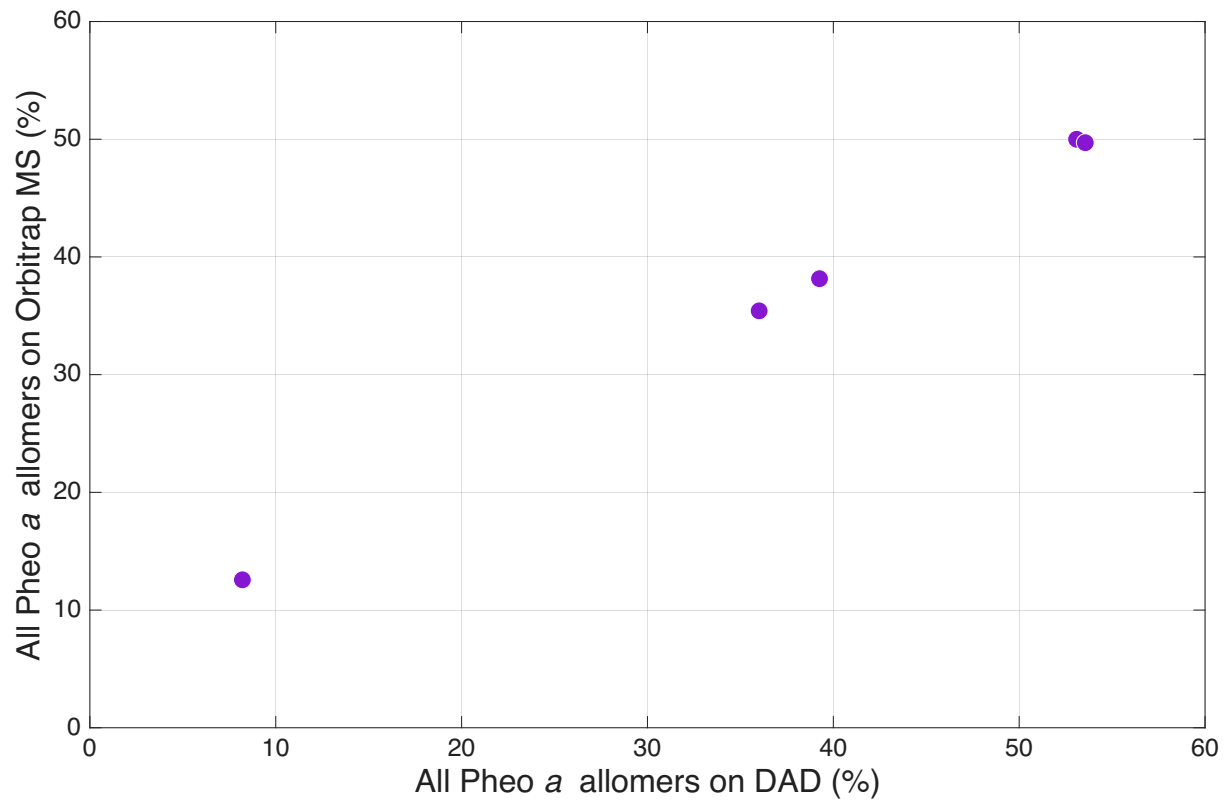
192



193

194 Figure S4

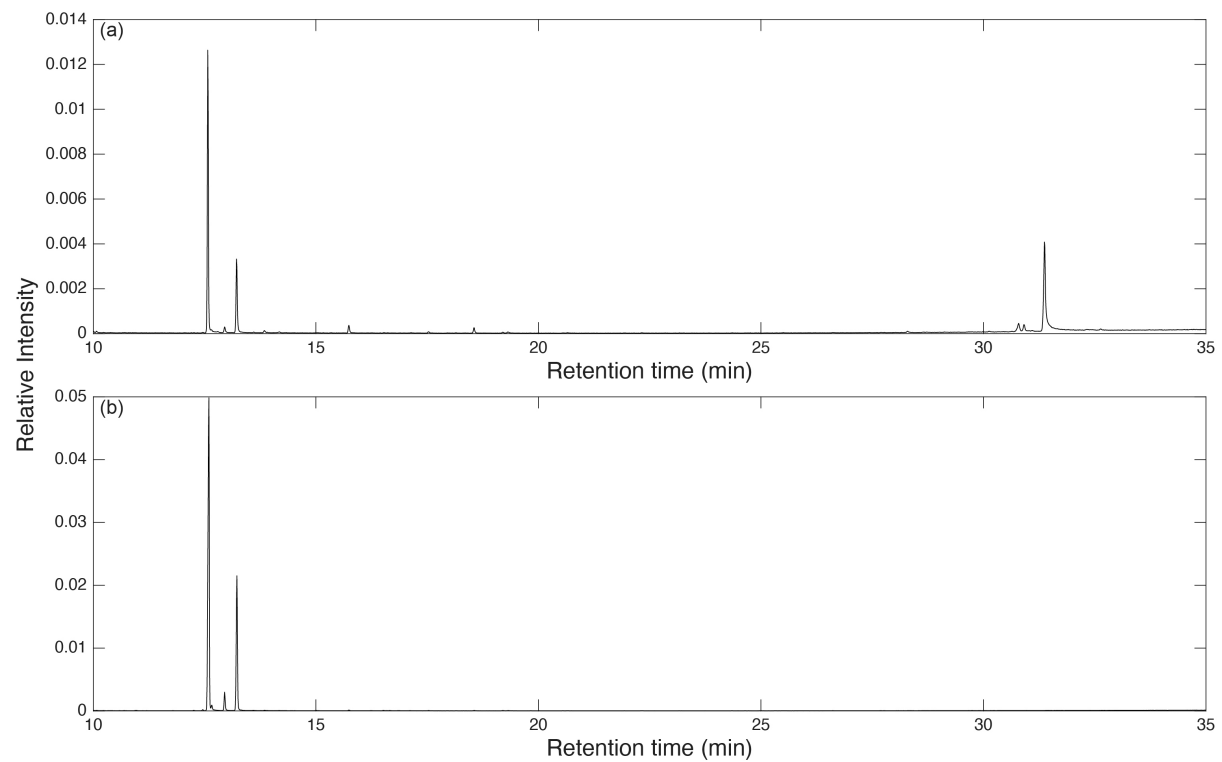
195



196

197 Figure S5

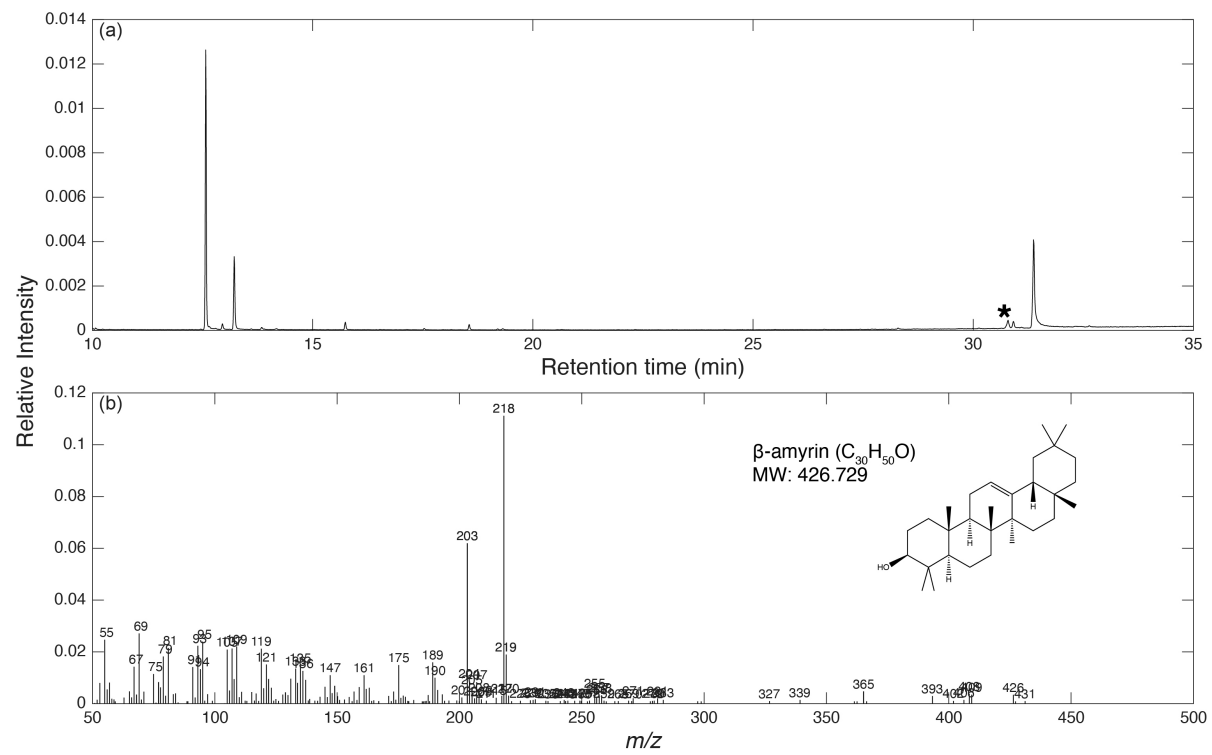
198



199

200 Figure S6

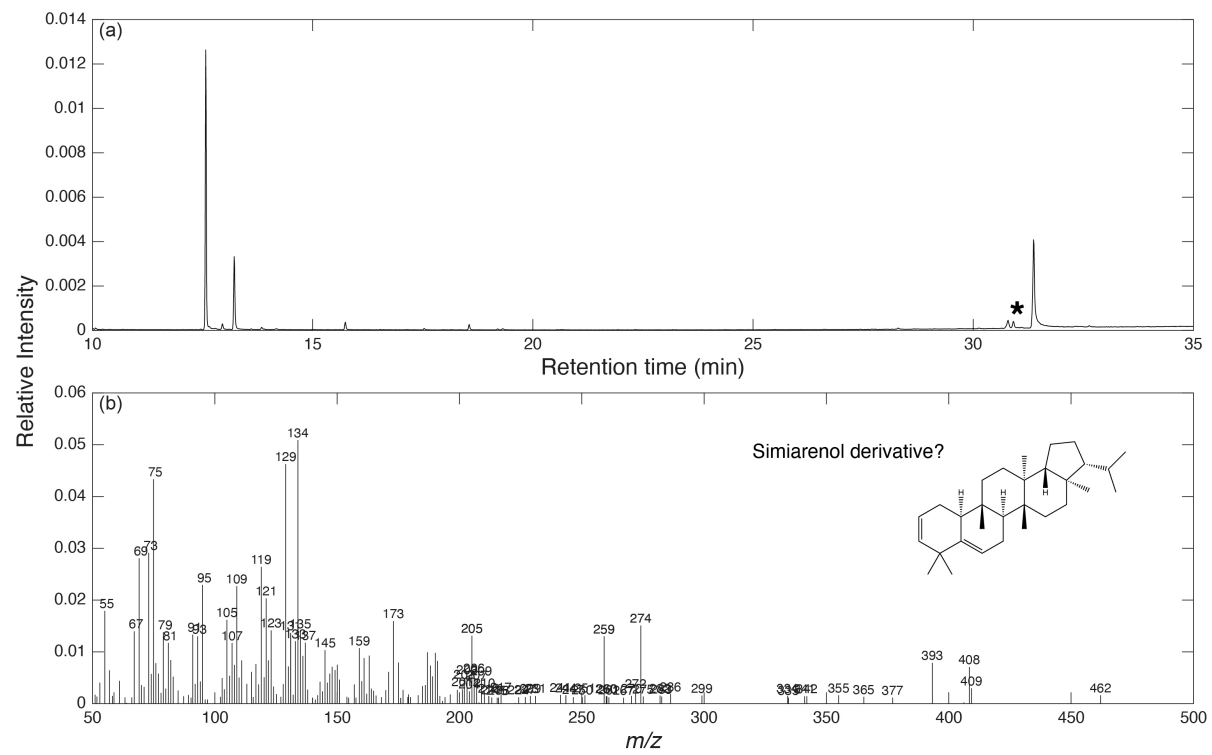
201



202

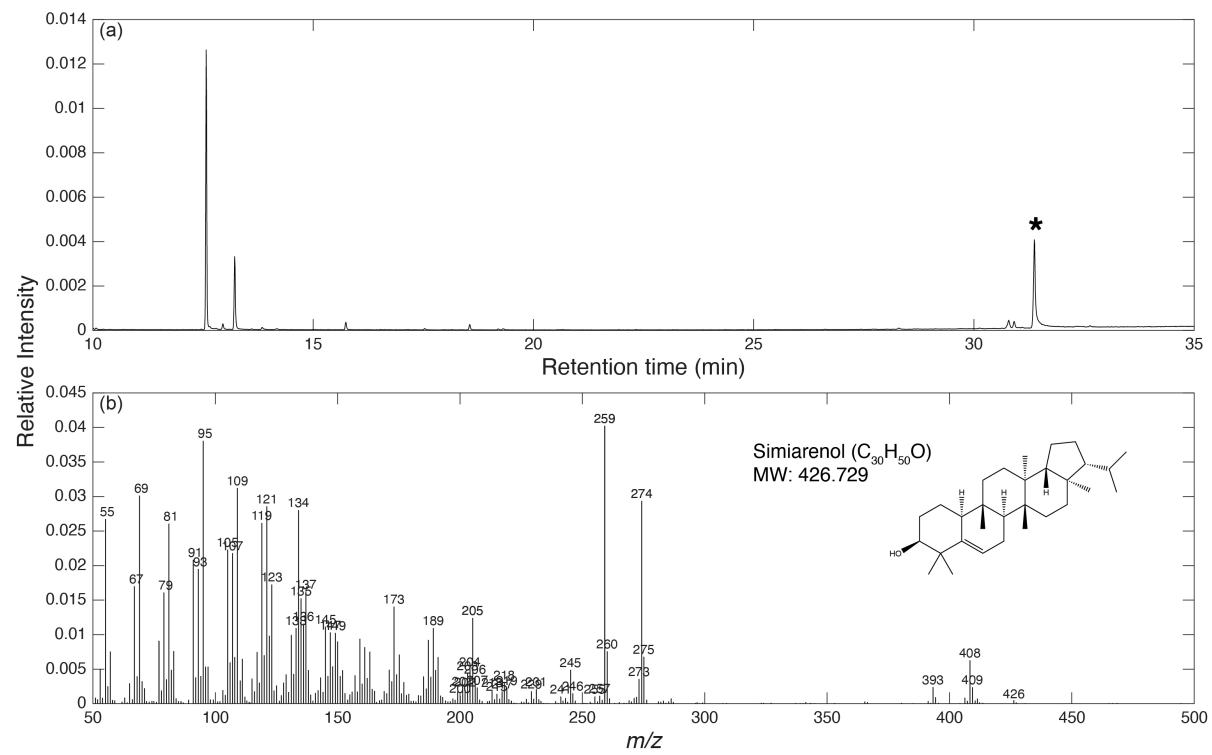
203 Figure S7

204



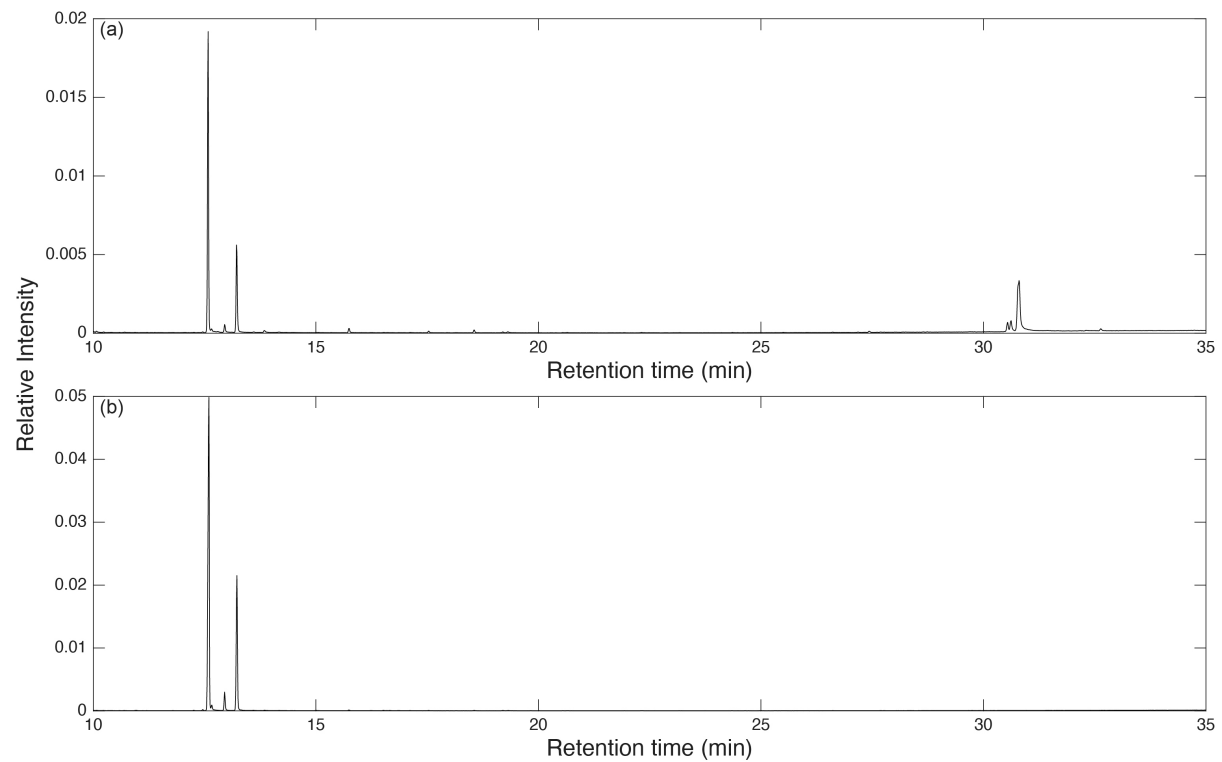
206 Figure S8

207



209 Figure S9

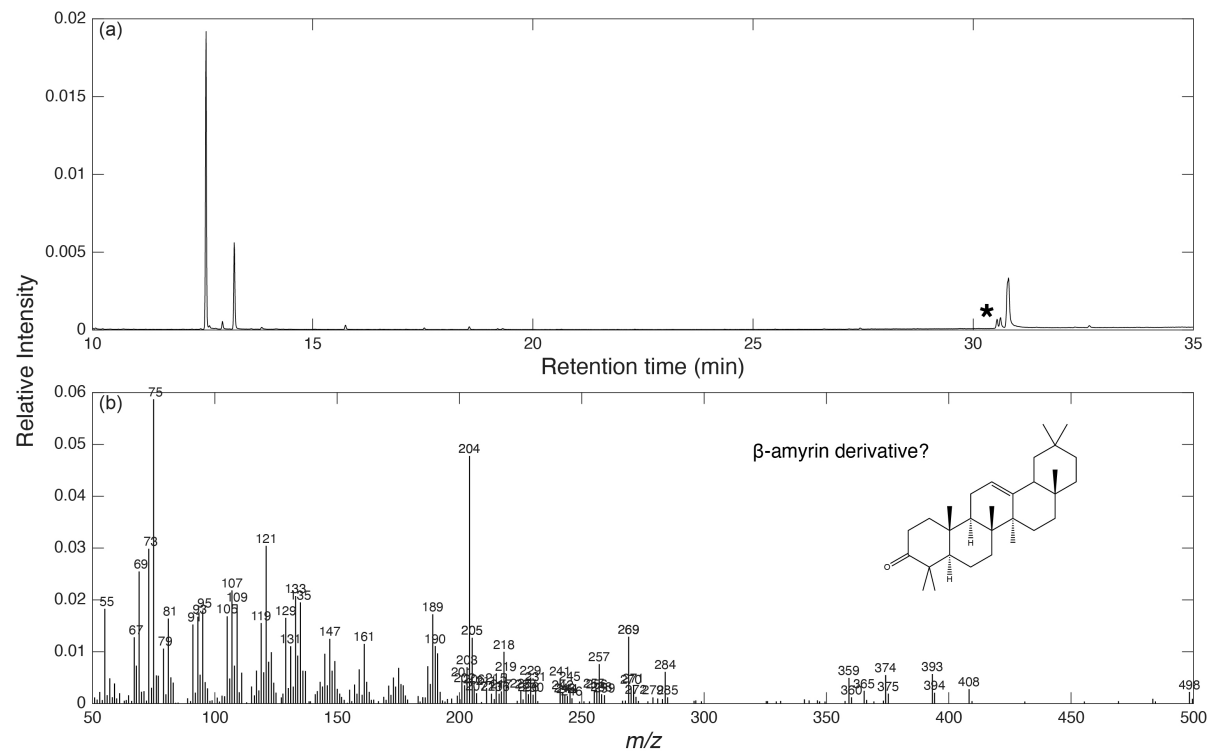
210



211

212 Figure S10

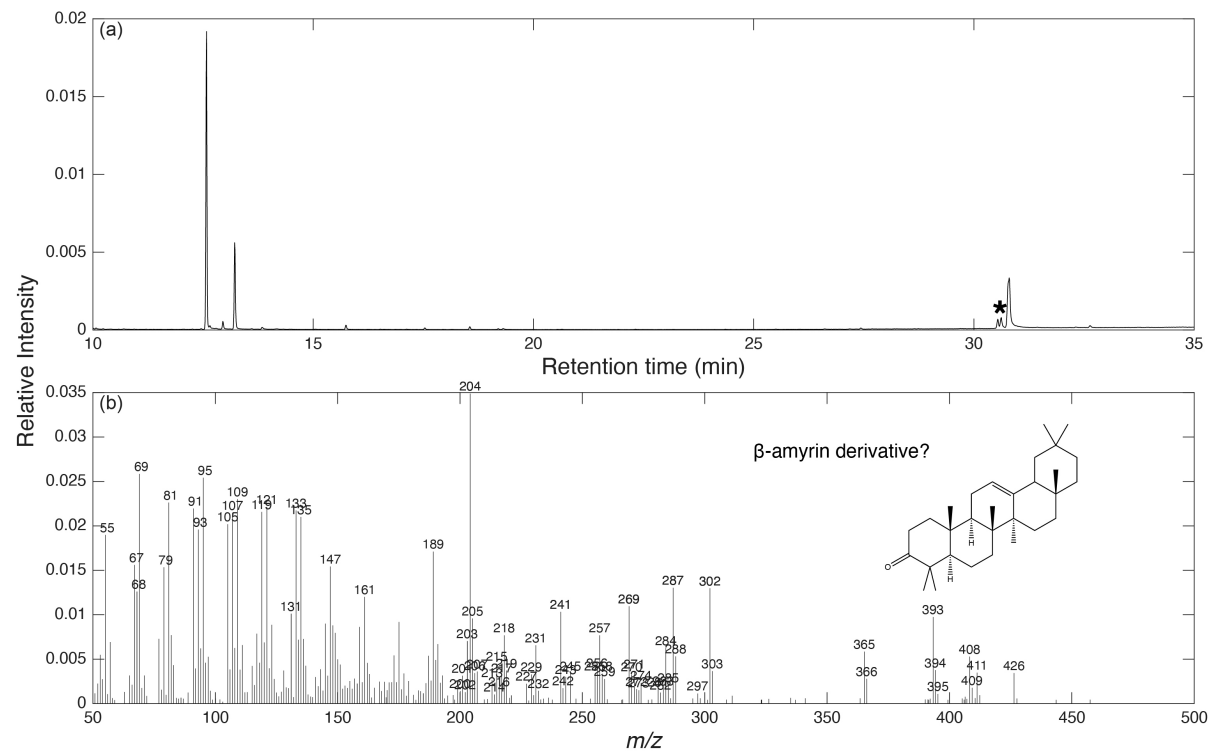
213



214

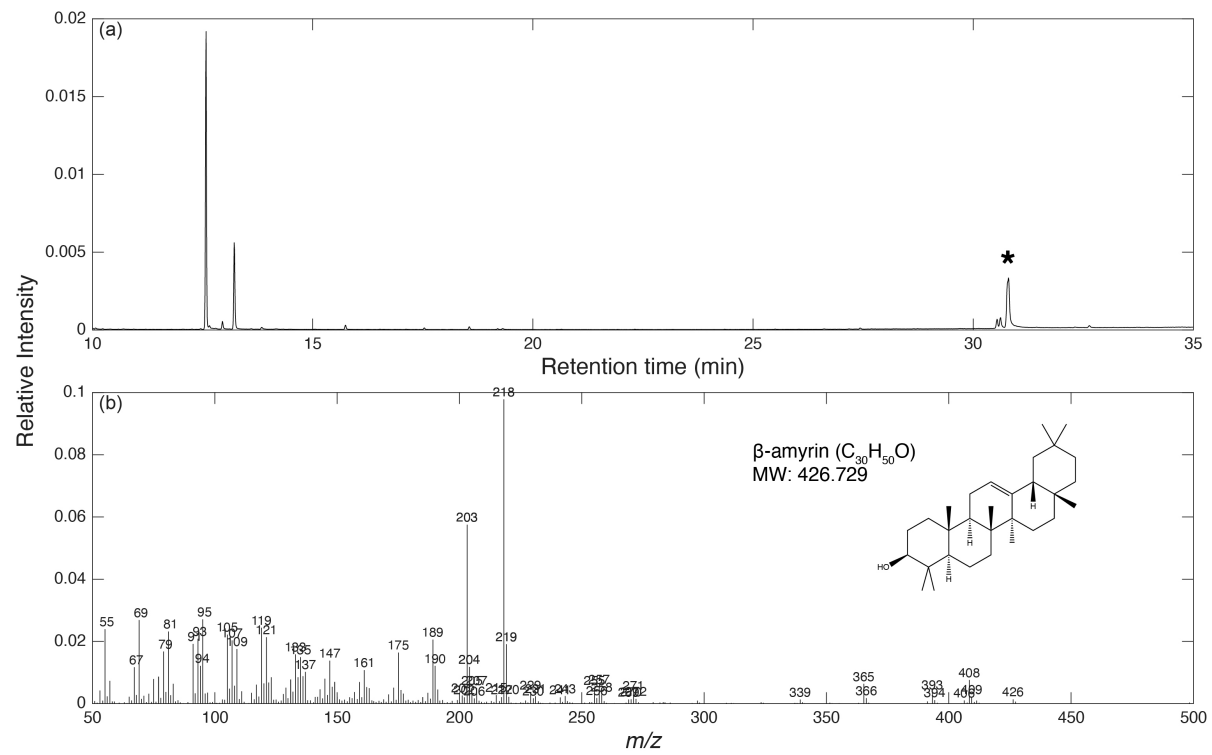
215 Figure S11

216



218 Figure S12

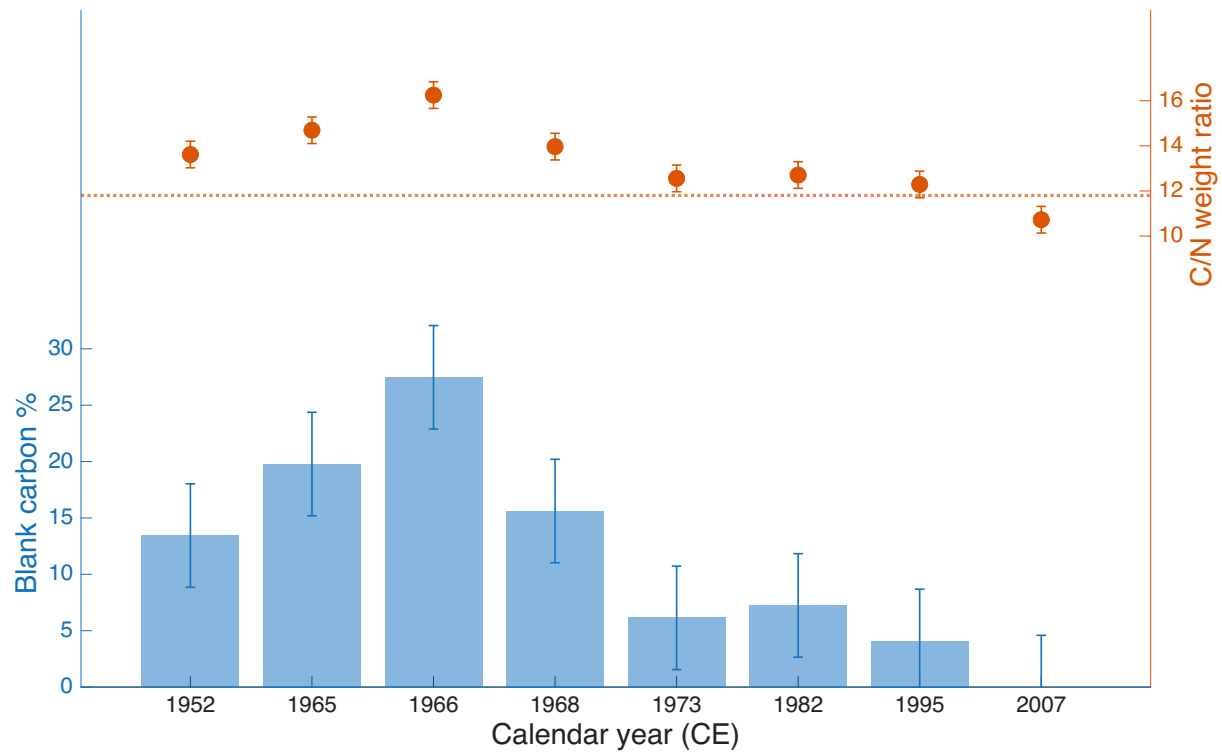
219



220

221 Figure S13

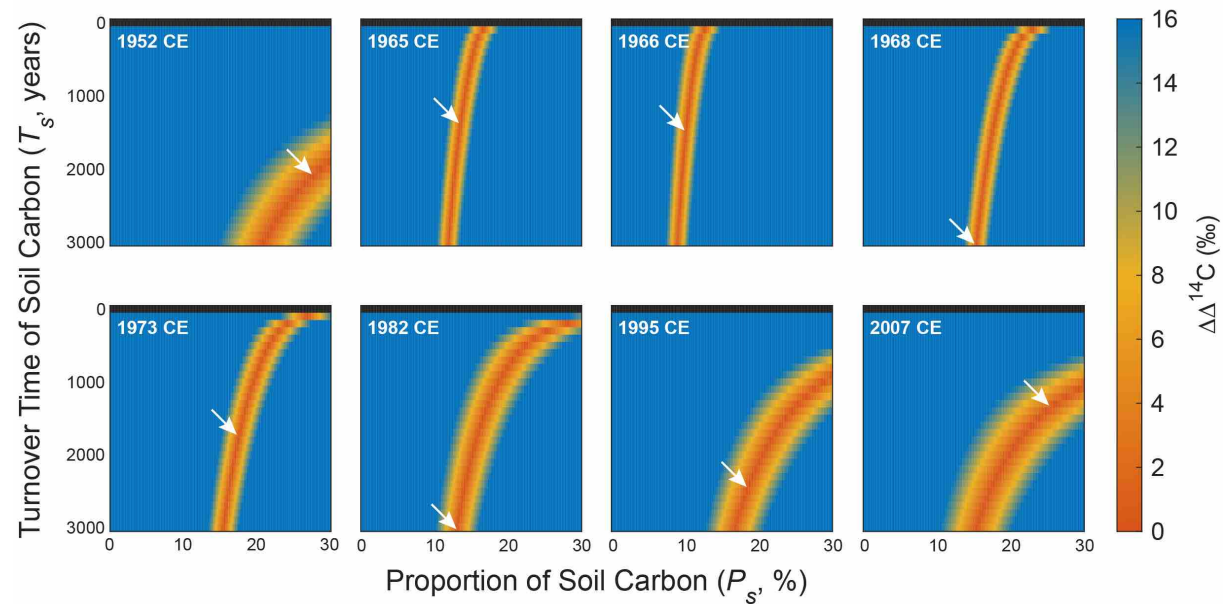
222



223

224 Figure S14

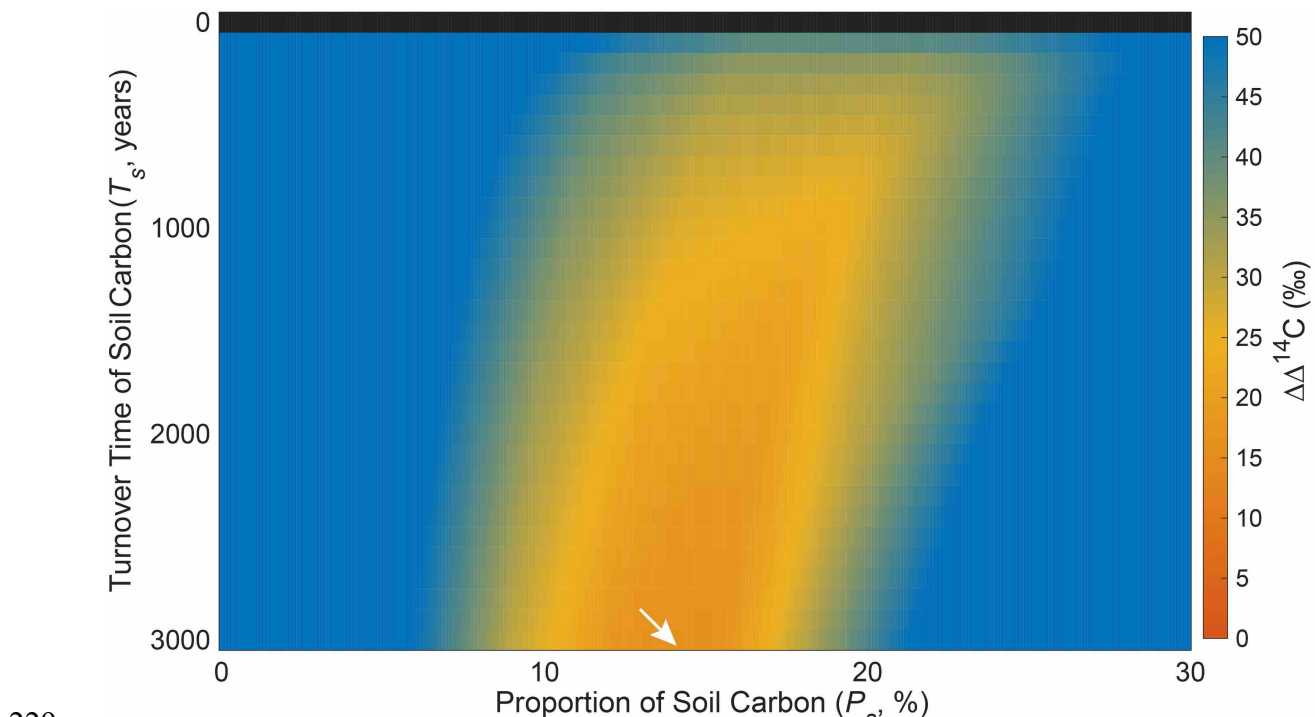
225



226

227 Figure S15

228



229

230 Figure S16